



## Utilization of volcanic ashes for the production of geopolymers cured at ambient temperature



H.K. Tchakoute, A. Elimbi\*, E. Yanne, C.N. Djangang

Laboratoire de Physico chimie des Matériaux Minéraux, Université de Yaoundé 1, Faculté des Sciences, B.P. 812 Yaoundé, Cameroon

### ARTICLE INFO

#### Article history:

Received 21 October 2011

Received in revised form 11 January 2013

Accepted 16 March 2013

Available online 29 March 2013

#### Keywords:

Volcanic ash

Alkaline solution

Amorphous phase

Geopolymer

Ambient curing temperature

### ABSTRACT

Two types of volcanic ash were characterized (chemical and mineralogical compositions, amorphous phase composition, particle size distribution and specific surface area) and then used as raw materials for the synthesis of geopolymer cements cured at ambient temperature ( $24 \pm 3^\circ\text{C}$ ). The synthesized products were characterized by determination of setting time, 28-day compressive strength, X-ray diffraction and Fourier Transform Infrared Spectroscopy. The mineralogical composition, the amorphous phase composition, the particle size distribution, the specific surface area of the volcanic ashes as well as the molar ratios of  $\text{Na}_2\text{O}/\text{Al}_2\text{O}_3$  of the synthesized products and of  $\text{SiO}_2/\text{Na}_2\text{O}$  of the alkaline solutions were the main parameters which influenced the synthesis of geopolymers with attractive characteristics at ambient curing temperature. The volcanic ash sample whose mineralogical composition contained anhydrite, low content of free CaO, low specific surface area ( $2.3 \text{ m}^2/\text{g}$ ) and synthesized products with  $\text{Na}_2\text{O}/\text{Al}_2\text{O}_3$  molar ratios between 1.23 and 1.44 led to long setting time (test samples could be handled easily only after 14 days at ambient atmosphere of the laboratory) and low 28-day compressive strength (9–19 MPa) geopolymers. Moreover, its products swelled and presented cracks resulting from the formation of ettringite. The volcanic ash sample with large  $(\text{Al}_2\text{O}_3 + \text{SiO}_2)\%$  wt of amorphous phase, high specific surface area ( $15.7 \text{ m}^2/\text{g}$ ) and synthesized products with  $\text{Na}_2\text{O}/\text{Al}_2\text{O}_3$  molar ratios between 1.04 and 1.31 led to more effective geopolymers: setting time was between 490 and 180 min and 28-day compressive strength between 23 and 50 MPa at ambient curing temperature ( $24 \pm 3^\circ\text{C}$ ).

© 2013 Elsevier Ltd. All rights reserved.

### 1. Introduction

Geopolymers are prepared by alkaline activation of aluminosilicate materials such as calcined clays, certain industrial wastes and natural minerals or a mixture of such materials cured at ambient or slightly higher temperature [1]. The geopolymerization process depends on many parameters including chemical and mineralogical compositions, particle size distribution and specific surface area of the raw material, curing temperature, composition of alkaline solution, etc. Geopolymers are attractive for building materials, hazardous waste encapsulation, high strength, low shrinkage, low carbon emission, acid resistance, etc. [1,2].

The raw materials commonly used to synthesize geopolymers are fly ash, metakaolin, or certain industrial wastes [3–7]. Volcanic ashes are almost aluminosilicate-type whose percentage in  $\text{Al}_2\text{O}_3$  and  $\text{SiO}_2$  can allow their utilization in the synthesis of geopolymers [8]. An increasing number of researchers have been using volcanic ash as raw materials for the synthesis of geopolymers [9,10]. So far, geopolymer pastes synthesized from volcanic ash have either exhibited long setting time [11] or have not yet led to cement

pastes with compressive strength greater than 44 MPa when cured between 20 and  $40^\circ\text{C}$  [9,10]. This might result from chemical and mineralogical compositions of the used raw materials. The “Cameroon line” oriented N30°E is made up of volcanic units and volcano-plutonic complexes of tertiary age [12] whose activities have generated vast deposits of volcanic ash [13]. In Cameroon, little amount of this raw material is used as additive for the production of Portland cement, for improvement of the quality of untarred roads or as aggregate for concrete. The possibility of utilizing volcanic ash for the synthesis of effective geopolymers cured at ambient temperature could be of economic importance for countries with huge deposits of this raw material.

In this study, volcanic ashes were collected from two Cameroonian localities (Djoungo and Galim) and used in their natural state for the synthesis of geopolymers cured at ambient temperature ( $24 \pm 3^\circ\text{C}$ ). For this purpose, the volcanic ashes were characterized by determining their chemical and mineralogical compositions, chemical composition of amorphous phase, particle size distribution and specific surface area. Five alkaline solutions with  $\text{SiO}_2/\text{Na}_2\text{O}$  molar ratios between 0.7 and 1.4 were prepared and used as activators for the synthesis of geopolymer cement pastes. The products were characterized by determination of setting time and 28-day compressive strength. Hardened geopolymer cement

\* Corresponding author. Tel.: +237 77 61 26 23; fax: +237 22 23 44 96.

E-mail address: [aelimbi2002@yahoo.fr](mailto:aelimbi2002@yahoo.fr) (A. Elimbi).

paste powders were also submitted to X-ray diffraction and Fourier Transform Infrared analysis.

## 2. Materials and experimental methods

### 2.1. Materials

The volcanic ashes originate from Djoungo and Galim, two localities along the “Cameroon line” [12]. They are vesicular particles of low density and various forms and they are referenced as  $Z_D$  (volcanic ash from Djoungo) and  $Z_G$  (volcanic ash from Galim).  $Z_D$  is dark-red and partially used for improvement of the quality of untarred roads or as additive for the production of Portland cement.  $Z_G$  particles are black and the local population commonly uses them as aggregate for concrete. The collected samples were washed with distilled water, dried at 105 °C for 72 h, ground and then sieved to 80  $\mu\text{m}$ . A brick-red powder was obtained from  $Z_D$  and a grey powder from  $Z_G$ .

The alkaline solution was a mixture of an aqueous solution of sodium hydroxide (12 M) and sodium silicate with bulk density of 1400 kg/m<sup>3</sup>. The sodium hydroxide solution was obtained by dissolving sodium hydroxide pellets of 99% purity in distilled water. The sodium silicate solution was made up of 28.7% SiO<sub>2</sub>, 8.9% Na<sub>2</sub>O and 62.4% H<sub>2</sub>O by weight. In order to determine the most convenient alkaline activating solution for effective geopolymers, five mixtures with SiO<sub>2</sub>/Na<sub>2</sub>O molar ratios of 0.7, 0.9, 1.1, 1.3 and 1.4 were prepared. Before use, the alkaline activating solutions were stored at ambient temperature (24 ± 3 °C) for at least 24 h.

### 2.2. Experimental methods

The chemical analyses were carried out by Inductive Coupled Plasma-Atomic Emission Spectrometry. The crystalline phases were determined by X-ray diffraction using a Philip PW 3050/60 diffractometer, operating by reflexion of  $K_{\alpha 1}$  radiation of Cu. The particle size distribution was performed using a courter LS 130 and the specific surface area by BET method using a Micromeritics Flowsorb ASAP 202. The amorphous phase content was determined by a method performed by Segalen [14]. Determination of the chemical composition of amorphous phase consisted of subtracting the content of dried unreacted matter via Segalen's method from the bulk composition. Cement pastes were obtained by mixing powder of volcanic ashes and alkaline activating solution for 10 min in a Hobart mixer (*M&O, modèle N50-G*). In order to get mixtures of good workability, the liquid/solid mass ratios were 0.49 (products from  $Z_G$ ) and 0.37 (products from  $Z_D$ ). Since the alkaline solutions were of SiO<sub>2</sub>/Na<sub>2</sub>O molar ratios 0.7, 0.9, 1.1, 1.3 and 1.4, the cement pastes produced were labeled as  $Z_{D7}$ ,  $Z_{D9}$ ,  $Z_{D11}$ ,  $Z_{D13}$  and  $Z_{D14}$  ( $Z_D$ -based geopolymers) and  $Z_{G7}$ ,  $Z_{G9}$ ,  $Z_{G11}$ ,  $Z_{G13}$  and  $Z_{G14}$  ( $Z_G$ -based geopolymers). Fresh pastes were molded in cylindrical PVC moulds (diameter 31 mm; height 62 mm). Once molded, they were vibrated for 10 min on an electrical vibrating table (*M & O, type 202, N°106*) to remove entrapped air bubbles, then covered with a thin film of polyethylene to avoid water evaporation and later on cured at ambient temperature (24 ± 3 °C) for 24 h before demolding (except the  $Z_D$ -based geopolymers which needed more days for consolidation). Setting time was measured using the Vicat apparatus according to the EN 196-3 standard. Compressive strength was determined on hardened geopolymer cement cylinder paste samples aged of 28 days using an electro-hydraulic press (*M & O, type 11.50, N°21*) at an average rate of 3 mm/min. Fourier Transform Infrared Spectroscopy was performed on powders of  $Z_D$  and  $Z_G$  and 28-day geopolymers with the aid of a Bruker Alpha-p, operating in absorbance mode.

**Table 1**

Chemical composition of the volcanic ashes (LOI = loss on ignition).  $Z_D$ : volcanic ash from Djoungo region and  $Z_G$ : volcanic ash from Galim region.

Oxides (%)	$Z_D$	$Z_G$
SiO <sub>2</sub>	44.04	41.36
Al <sub>2</sub> O <sub>3</sub>	15.26	15.41
Fe <sub>2</sub> O <sub>3</sub>	12.77	12.88
TiO <sub>2</sub>	2.87	3.04
MnO	0.17	0.2
MgO	7.00	6.45
CaO	9.29	7.88
K <sub>2</sub> O	1.35	0.90
Na <sub>2</sub> O	5.64	2.22
SO <sub>3</sub>	0.01	Trace
P <sub>2</sub> O <sub>5</sub>	0.53	0.48
Cr <sub>2</sub> O <sub>3</sub>	0.02	0.03
LOI	1.1	9.31
SiO <sub>2</sub> /Al <sub>2</sub> O <sub>3</sub> (molar ratio)	4.90	4.55
(SiO <sub>2</sub> + Al <sub>2</sub> O <sub>3</sub> )	59.30	56.77
Total	100.04	100.10

**Table 2**

Chemical composition of amorphous phase of the volcanic ashes, % wt.

Volcanic ashes	$Z_D$	$Z_G$
Al <sub>2</sub> O <sub>3</sub>	5.31	11.15
SiO <sub>2</sub>	15.33	25.80
CaO	3.23	5.11
Other oxides + organic matter	10.93	22.74
Total	34.8	64.8

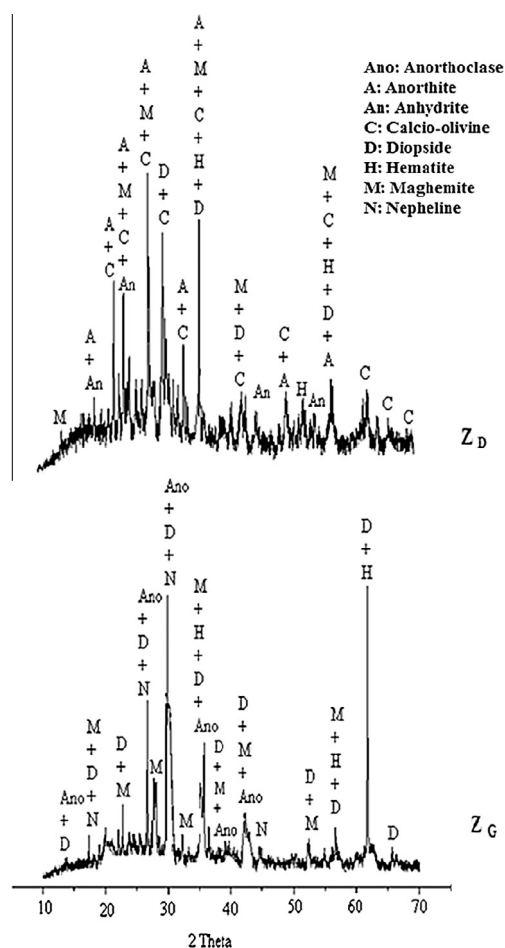


**Fig. 1.** X-ray diffractograms of the volcanic ashes.

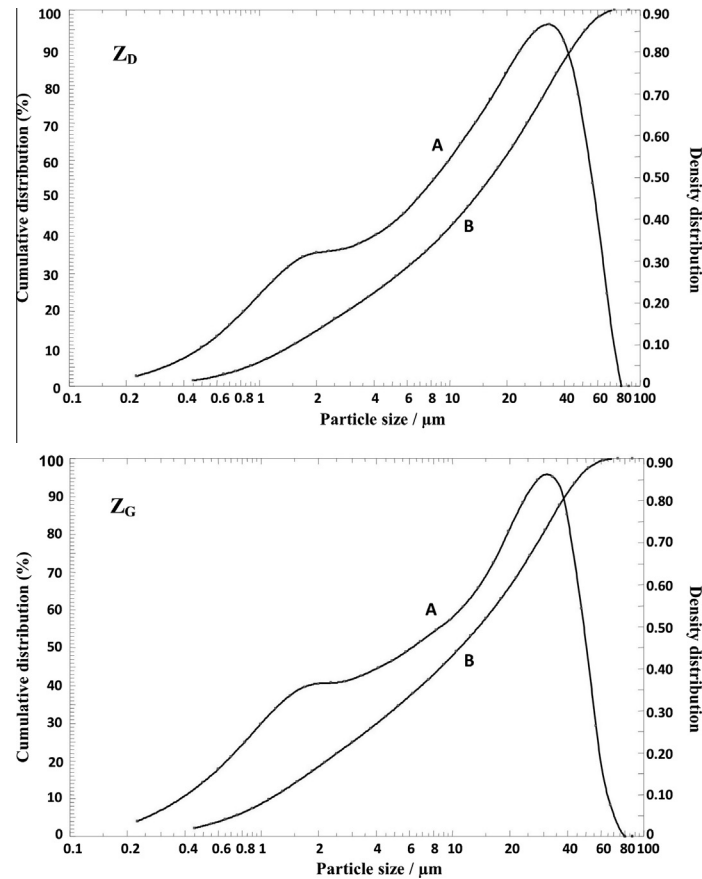


Fig. 2. Particle size distribution of the volcanic ashes (A: density distribution; B: cumulative distribution).

### 3. Results and discussion

#### 3.1. Characteristics of volcanic ashes

The chemical composition of the volcanic ashes is summarized in Table 1. The  $\text{SiO}_2/\text{Al}_2\text{O}_3$  molar ratio is 4.90 for  $Z_D$  and 4.55 for  $Z_G$  and the sum ( $\text{SiO}_2 + \text{Al}_2\text{O}_3$ ) is 59.4% wt for  $Z_D$  and 56.8% wt for  $Z_G$ . These values are among the basic ingredients of raw materials used for geopolymer synthesis and are contained in the intervals reported by Davidovits [3] and Palomo et al. [4]. Calcium oxide content has been reported to have a significant influence on the properties of geopolymer cements [15,16] and is 9.29% wt for  $Z_D$  and 7.88% wt for  $Z_G$ . Loss on ignition is 1.1% wt ( $Z_D$ ) and 9.3% wt ( $Z_G$ ) which may likely indicate presence of organic matter in  $Z_G$ . The chemical composition and amount of amorphous phase of  $Z_D$  and  $Z_G$  are given in Table 2. It is evident that presence of amorphous phase with great content of ( $\text{SiO}_2 + \text{Al}_2\text{O}_3$ )% wt in an aluminosilicate is beneficial for the synthesis of geopolymers [15,17,18]. Thus,  $Z_G$ -based geopolymers could be more effective than those of  $Z_D$ -based geopolymers. On the other hand, the greater content of free CaO in  $Z_G$  than in  $Z_D$  may allow lower setting time in the  $Z_G$ -based geopolymers [18]. By the contrast, the low content of free CaO indicates that calcium belongs mostly to the composition of  $Z_D$  crystalline phases (Tables 1 and 2). In addition to maghemite, hematite and diopside that are common minerals to these volcanic ashes,  $Z_D$  also contains calcio-olivine, anorthite and anhydrite and  $Z_G$  anorthoclase and nepheline (Fig. 1). The particle size distribution ranges from 0.23 to 80  $\mu\text{m}$ , the mode is around 35  $\mu\text{m}$  ( $Z_D$ ) and 32  $\mu\text{m}$  ( $Z_G$ ) and the average particle size ( $d_{50}$ ) is 13.01 and 10.68  $\mu\text{m}$  respectively for  $Z_D$  and  $Z_G$  (Fig. 2). The specific surface area is 2.3  $\text{m}^2/\text{g}$  for  $Z_D$  and 15.7  $\text{m}^2/\text{g}$  for  $Z_G$ . These results indicate

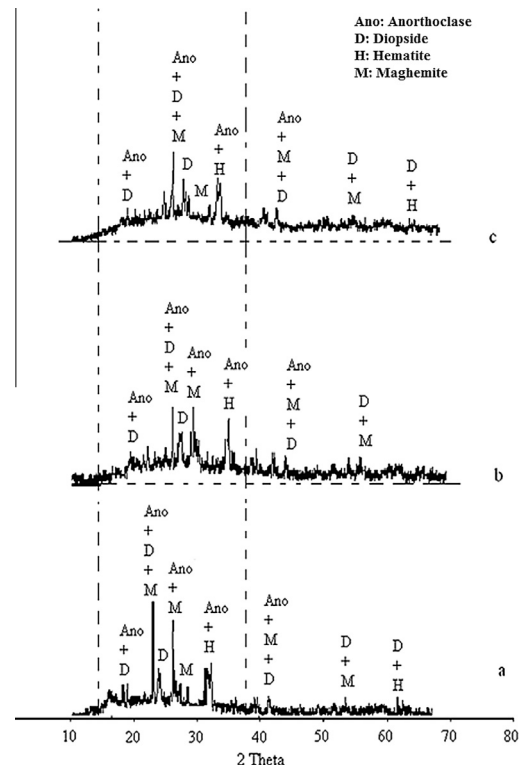


Fig. 3. X-ray diffractograms of the  $Z_G$ -based geopolymers ( $a = Z_{G7}$ ;  $b = Z_{G11}$ ;  $c = Z_{G14}$ ).

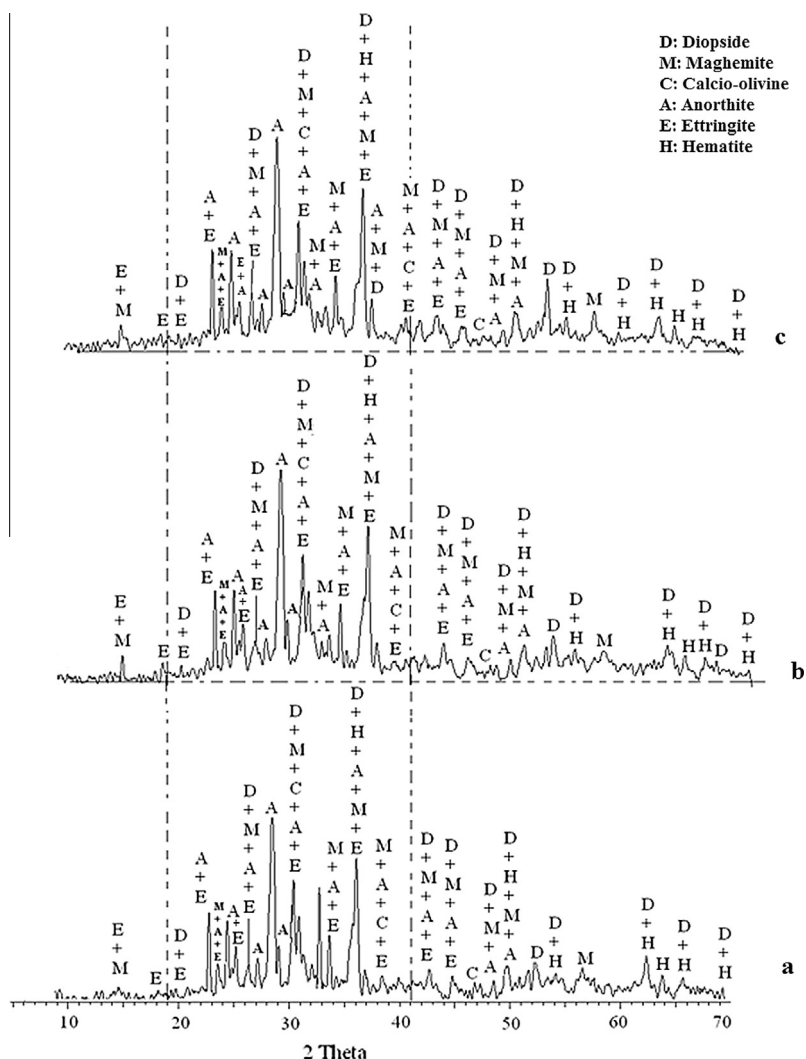


Fig. 4. X-ray diffractograms of the  $Z_D$ -based geopolymers ( $a = Z_{D7}$ ;  $b = Z_{D11}$ ;  $c = Z_{D14}$ ).

good correlation between the particle size distribution and the specific surface area, i.e. the finer the particles, the greater the specific surface area. The greater specific surface area exhibited by  $Z_C$  by comparison with  $Z_D$  may result from presence of more porous microstructure of  $Z_C$  particles. Particle size distribution is one of the important physical parameters impacting on geopolymer synthesis of aluminosilicates as well as on resulting products since a significant part of reaction occurs at the particle–liquid interface [19]. Thus for a given aluminosilicate raw material, the smaller and the more porous microstructure particles, the greater the specific surface area and the more it is activated in alkaline medium. All these results suggested that the  $Z_C$ -based geopolymers could be more effective than the  $Z_D$ -based geopolymers.

### 3.2. Characteristics of geopolymers

#### 3.2.1. X-ray diffraction

Figs. 3 and 4 show the X-ray diffraction patterns of the geopolymers. Except anhydrite and nepheline, all the crystalline phases observed are the same as those present in  $Z_D$  and  $Z_C$  (Figs. 1, 3 and 4). The presence of ettringite ( $6\text{CaO} \cdot \text{Al}_2\text{O}_3 \cdot 3\text{SO}_3 \cdot 31\text{H}_2\text{O}$ ) in the  $Z_D$ -based geopolymers originates from the chemical reaction between anhydrite ( $\text{CaSO}_4$ ) and  $[\text{Al}(\text{OH})_4]^-$  complex resulting from dissolution of the raw material in alkaline medium [20]. The absence of nepheline in the  $Z_C$ -based geopolymers indicates that it has reacted. In fact, nepheline is an aluminosilicate. The halo peak

between  $18^\circ$  and  $40^\circ$  is characteristic of amorphous phase of geopolymers. However the area under each halo peak of the diffractograms increases with the  $\text{SiO}_2/\text{Na}_2\text{O}$  molar ratio of the alkaline solutions (Figs. 3 and 4). It seems as if there exists a correlation between this area and the amount of amorphous phase contained in the geopolymers. In fact, an increase of the  $\text{SiO}_2/\text{Na}_2\text{O}$  molar ratio of the alkaline solution promotes the polycondensation stage of the geopolymer synthesis [21].

#### 3.2.2. FTIR spectra

Figs. 5 and 6 show the FTIR results of the volcanic ashes and the geopolymers. The spectra of  $Z_D$  and  $Z_C$  (Figs. 5a and 6a) exhibit two main absorption domains and those of the geopolymers three (Figs. 5b–d and 6b–d). The first absorption band is a sharp peak at  $2360\text{ cm}^{-1}$  and concerns the geopolymers. This peak is characteristic of stretching vibrations of  $-\text{OH}$  under strong hydrogen bonding [21], which gives evidence of adsorbed water in the geopolymers. The second domain is made up of two absorption bands, one at  $1650\text{ cm}^{-1}$  and the other at  $1540\text{ cm}^{-1}$ . Both indicate the  $\text{H}-\text{O}-\text{H}$  bending vibrations of water molecules [22]. The third domain contains an important absorption band around  $950\text{--}1000\text{ cm}^{-1}$  and is attributed to asymmetric stretching vibrations of  $\text{Si}-\text{O}-\text{Si}$  [23]. The intensity of this peak is high enough for volcanic ashes but is obviously reduced with the increasing of  $\text{SiO}_2/\text{Na}_2\text{O}$  molar ratio of alkaline solution as regards the geopolymers (Figs. 5b–d and 6b–d). This result seemed to indicate the rareness of  $\text{Si}-\text{O}-\text{Si}$

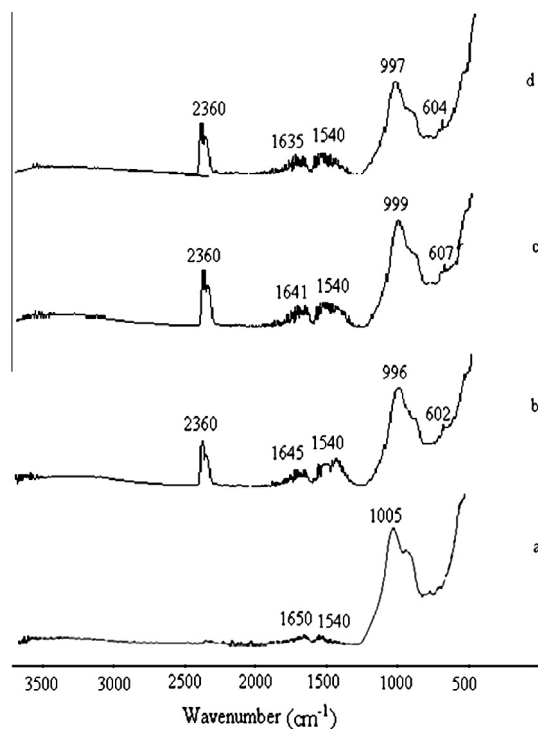


Fig. 5. IR spectra of the  $Z_G$ -based geopolymers ( $a = Z_G$ ;  $b = Z_{G7}$ ;  $c = Z_{G11}$ ;  $d = Z_{G14}$ ).

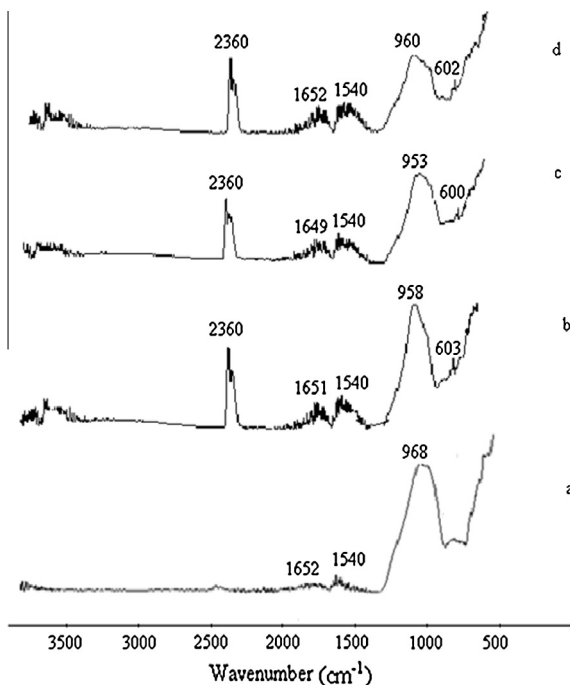


Fig. 6. IR spectra of the  $Z_D$ -based geopolymers ( $a = Z_D$ ;  $b = Z_{D7}$ ;  $c = Z_{D11}$ ;  $d = Z_{D14}$ ).

groups when the synthesis of geopolymers is on. The weak peak around  $600\text{ cm}^{-1}$  is ascribed to the symmetric stretching vibrations of Si–O–Al and Si–O–Si groups of the geopolymers [24].

### 3.2.3. Setting time

The  $Z_D$ -based geopolymers could be handled easily only after 14 days at ambient curing temperature ( $24 \pm 3^\circ\text{C}$ ). As a result of this, their setting time was not taken into account in Fig. 7. Setting time is generally influenced by parameters such as chemical com-

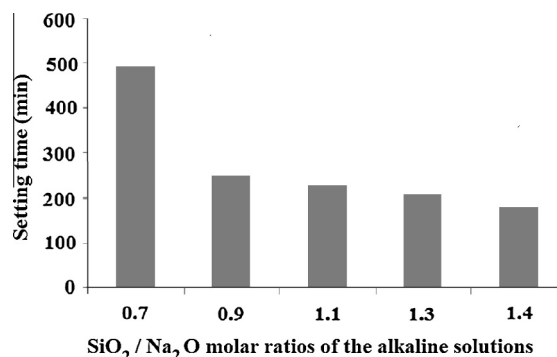


Fig. 7. Setting time of the  $Z_G$ -based geopolymers.

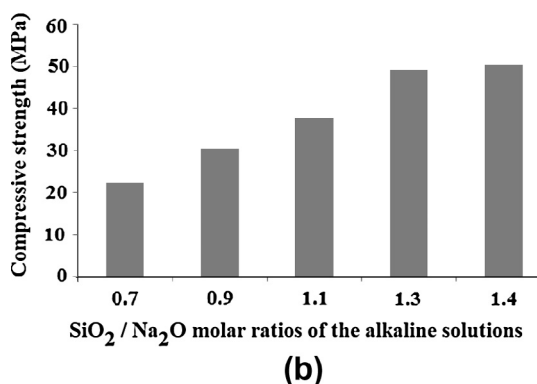
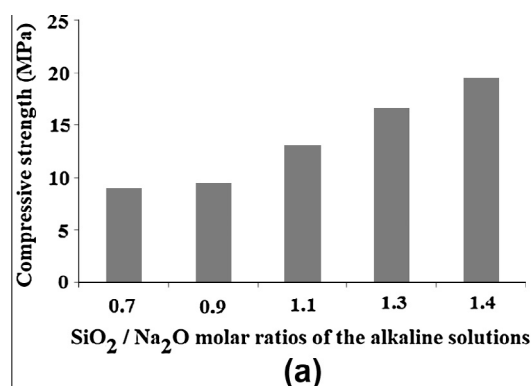


Fig. 8. Compressive strength of the  $Z_D$ -based geopolymers (a) and the  $Z_G$ -based geopolymers (b).

position and particle size distribution of raw material used for the synthesis of geopolymers [1]. Thus, long setting time of the  $Z_D$ -based geopolymer pastes could result from both low specific surface area ( $2.3\text{ m}^2/\text{g}$ ) and low content of free CaO (3.23% wt) of amorphous phase of  $Z_D$  particles. In fact, the lower the specific surface area and content of free CaO of an aluminosilicate, the higher the setting time of geopolymer pastes [17,18,25]. Elsewhere, setting time of the  $Z_G$ -based geopolymer pastes was between 490 and 180 min, and it decreased with the increase of  $\text{SiO}_2/\text{Na}_2\text{O}$  molar ratio of alkaline solutions. This result was in accordance with specific surface area ( $15.7\text{ m}^2/\text{g}$ ) and content of free CaO (5.11% wt) of  $Z_G$  particles along with the result obtained by Cheng and Chiu [26] who showed that the lower the  $\text{SiO}_2/\text{Na}_2\text{O}$  molar ratio, the higher the setting time.

### 3.2.4. Compressive strength

Fig. 8 shows the 28-day compressive strength of the geopolymers cured at ambient temperature ( $24 \pm 3^\circ\text{C}$ ) as a function of



**Table 3**  
Al<sub>2</sub>O<sub>3</sub>/SiO<sub>2</sub> and Na<sub>2</sub>O/Al<sub>2</sub>O<sub>3</sub> molar ratios of geopolymers.

Geopolymers	Z <sub>D7</sub>	Z <sub>D9</sub>	Z <sub>D11</sub>	Z <sub>D13</sub>	Z <sub>D14</sub>	Z <sub>G7</sub>	Z <sub>G9</sub>	Z <sub>G11</sub>	Z <sub>G13</sub>	Z <sub>G14</sub>
SiO <sub>2</sub> /Al <sub>2</sub> O <sub>3</sub>	5.43	5.55	5.64	5.70	5.75	5.26	5.41	5.52	5.60	5.66
Na <sub>2</sub> O/Al <sub>2</sub> O <sub>3</sub>	1.44	1.36	1.30	1.28	1.23	1.31	1.20	1.13	1.08	1.04

SiO<sub>2</sub>/Na<sub>2</sub>O molar ratio of the alkaline solutions. Compressive strength increased with increase of SiO<sub>2</sub>/Na<sub>2</sub>O molar ratio of the alkaline solutions. It is well known that increase of SiO<sub>2</sub>/Na<sub>2</sub>O molar ratio of alkaline activating solution results in acceleration of geopolymer synthesis and causes the reaction to proceed to a higher extent [26]. In addition, better strength properties are reported for geopolymers with SiO<sub>2</sub>/Al<sub>2</sub>O<sub>3</sub> molar ratios in the range of 3.0–3.8 and Na<sub>2</sub>O/Al<sub>2</sub>O<sub>3</sub> molar ratios of about 1 [27,28]. From the previous reports, it appeared that the synthesized geopolymers fell down with regard to their SiO<sub>2</sub>/Al<sub>2</sub>O<sub>3</sub> molar ratios but the sample Z<sub>G14</sub> as regards its Na<sub>2</sub>O/Al<sub>2</sub>O<sub>3</sub> molar ratio (Table 3). However, it is interesting to mention that the Z<sub>C</sub>-based geopolymers exhibited higher 28-day compressive strength values (23–50 MPa) than the Z<sub>D</sub>-based geopolymers (9–19 MPa) at ambient curing temperature (24 ± 3 °C). Although silica and alumina are among the main precursors for the geopolymer reaction, there are other characteristics of raw materials and of synthesized products that play significant roles to get high compressive strength values. Among them are the composition of amorphous phase (Table 2), the average particle size (13.01 µm for Z<sub>D</sub> and 10.68 µm for Z<sub>C</sub>), the specific surface area (2.3 m<sup>2</sup>/g for Z<sub>D</sub> and 15.7 m<sup>2</sup>/g for Z<sub>C</sub>) as well as the Na<sub>2</sub>O/Al<sub>2</sub>O<sub>3</sub> molar ratios of the geopolymers (Table 3). In fact, during the reaction between volcanic ash and alkaline solutions, the higher the content of (Al<sub>2</sub>O<sub>3</sub> + SiO<sub>2</sub>)% wt of amorphous phase, the higher the amount of [Si(OH)<sub>3</sub>]<sup>−</sup> and [Al(OH)<sub>4</sub>]<sup>−</sup> intermediate complexes released at the stage of dissolution of the aluminosilicate [19]. This allows the formation of a large amount of geopolymer binder that leads to high 28-day compressive strength values. The particle size also affects geopolymerization reaction: the finer the particle size the greater the specific surface area and the more reactive the raw material [19]. The low 28-day compressive strength values of the Z<sub>D</sub>-based geopolymers might also be attributed to the swelling and the presence of cracks which appeared in the products few days after demoulding. These cracks resulted from presence of ettringite in the geopolymers [22,29]. In fact, presence of ettringite is attributed to the chemical reaction between anhydrite (Fig. 1) and [Al(OH)<sub>4</sub>]<sup>−</sup> intermediate complex formed during dissolution of volcanic ashes in alkaline medium. Greater compressive strength values may be expected from volcanic ash-based geopolymers via slight increase of curing temperature [9].

#### 4. Conclusion

This study investigated the utilization of two types of volcanic ash to produce geopolymers cured at ambient temperature. The properties of the synthesized products were dependent on certain characteristics of the raw materials. The volcanic ash sample with low specific surface area and low content of free CaO led to geopolymers with long setting time. On the other hand, the formation of ettringite generated swelled products with cracks which led to low compressive strength (9–19 MPa). The volcanic ash sample with great specific surface area and important (Al<sub>2</sub>O<sub>3</sub> + SiO<sub>2</sub>)% wt of amorphous phase gave geopolymers with compressive strength between 23 and 50 MPa. Although the SiO<sub>2</sub>/Al<sub>2</sub>O<sub>3</sub> molar ratios of the investigated geopolymers were greater than those reported by literature to give better properties, it was possible to get Na<sub>2</sub>O/Al<sub>2</sub>O<sub>3</sub> molar ratios giving attractive geopolymers. Anyway,

volcanic ash has the potential to be raw material for geopolymer synthesis.

#### Acknowledgments

The authors would like to express special thanks to Dr. Elie Kamseu and Mr. Jean Aimé Mbey for carrying out ICP-AES, XRD, particle size distribution and BET analysis.

#### References

- [1] Komnitas K, Zaharakis D. Geopolymerisation: a review and prospects for the minerals industry. *Miner Eng* 2007;20(13):1261–77.
- [2] Duxson P, Fernandez-Jimenez A, Provis JL, Lukey GC, Palomo A, Van Deventer JSJ. Geopolymer technology: the current state of the art. *J Mater Sci* 2007;42(9):2917–33.
- [3] Davidovits J. Geopolymers: inorganic polymeric new materials. *J Mater Educ* 1994;16(2–3):91–139.
- [4] Palomo A, Grutzeit MW, Blanco MT. Alkali-activated fly ashes: cement for the future. *Cem Concr Res* 1999;29(8):1323–9.
- [5] Bell JL, Driemeyer PE, Kriven WM. Formation of ceramics from metakaolin-based geopolymers. Part II. K-based geopolymer. *J Am Ceram Soc* 2009;92(3):607–15.
- [6] Temuujin J, Williams RP, Van-Riessen A. Effect of mechanical activation of fly ash on the properties of geopolymer cured at ambient temperature. *J Mater Proc Technol* 2009;209(12–13):5276–80.
- [7] Muñiz-Villarreal MS, Manzano-Ramírez A, Sampieri-Bulbarela S, Ramón Gasca-Tirado J, Reyes-Araiza JL, Rubio-Ávalos JC, et al. The effect of temperature on the geopolymerization process of a metakaolin-based geopolymer. *Mater Lett* 2011;65(6):995–8.
- [8] Kamseu E, Leonelli C, Perera DS, Melo UC, Lemougna PN. Investigation of volcanic ash-based geopolymers as potential building materials. *Inter Ceram* 2009;58(2):136–40.
- [9] Bondar D, Lynsdale CJ, Milestone NB, Hassani N, Ramezaniapour AA. Effect of heat treatment on reactivity-strength of alkali-activated natural pozzolans. *Constr Build Mater* 2011;25(10):4065–71.
- [10] Bondar D, Lynsdale CJ, Milestone NB, Hassani N, Ramezaniapour AA. Effect of type, form, and dosage of activators on strength of alkali-activated natural pozzolans. *Cem Concr Compos* 2011;33(2):251–60.
- [11] Allahverdi A, Mehrpour K, Kani EN. Taftan pozzolan-based geopolymer cement. *Int J Eng Sci* 2008;19(3):1–5 (special issue).
- [12] Kamdem JB, Kraml M, Keller J, Henjes-kunt F. Cameroon line magmatism: conventional K/Ar and single-crystal laser <sup>40</sup>Ar/<sup>39</sup>Ar ages of rocks and minerals from the hosierr nigo anarogenic complex, Cameroon. *J Afri Earth Sci* 2002;35(1):99–105.
- [13] Leonelli C, Kamseu E, Boccaccini DN, Melo UC, Rizzuti A, Billong N, et al. Volcanic ash as alternative raw materials for traditional vitrified ceramic products. *Adv Appl Ceram* 2007;106(1):1–7.
- [14] Segalen P. Note sur une méthode de détermination des produits minéraux amorphes dans certains sols à hydroxydes tropicaux. *Cahier ORSTOM Série Pédol* 1968;6(1):105–26.
- [15] Van Jaarsveld JGS, Van Deventer JSJ, Lukey GC. The characterisation of source materials in fly ash-based geopolymers. *Mater Lett* 2003;57(7):1272–80.
- [16] Xu H, Lukey GC, Van Deventer JSJ. The activation of class C-, class F-fly ash and blast furnace slag using geopolymerisation. In: Malhotra VM, editor. Proceedings of the 8th CANMET/ACI international conference on fly ash, silica fume, slag, and natural pozzolans in concrete, Las Vegas, USA. p. 797–820.
- [17] Williams R. Characterisation of fly ash for production of geopolymer. PhD thesis. Perth, Curtin University of Technology; 2006.
- [18] Temuujin J, Van Riessen A, Williams R. Influence of calcium compounds on the mechanical properties of fly ash geopolymer pastes. *J Hazard Mater* 2009;167(1–3):82–8.
- [19] Diaz EI, Allouche EN, Eklund S. Factors affecting the suitability of fly ash as source material for geopolymers. *Fuel* 2010;89(5):992–6.
- [20] Aubert JE. Utilisation de déchets dans les bétons: exemple des cendres volantes d'incinérateurs d'ordures ménagères, 21ème rencontres universitaires de génie civil-prix René Houpert, Toulouse, France; 2003. p. 11–20.
- [21] Maragkos I, Giannopoulou IP, Panias D. Synthesis of ferronickel slag-based geopolymers. *Miner Eng* 2009;22(2):196–203.

- [22] Lee WKW, Van Deventer JSJ. Structural reorganisation of class F fly ash in alkaline silicate solution. *Colloid Surf A* 2002;211(1):49–66.
- [23] Villa C, Pecina ET, Torres R, Gomez L. Geopolymer synthesis using alkaline activation of natural zeolite. *Constr Build Mater* 2010;24(11):2084–90.
- [24] Davidovits J. Chemistry of geopolymeric systems terminology. In: *Proceedings of geopolymer '99 international conference*, Saint Quentin, France; 1999. p. 9–40.
- [25] Weng L, Sagoe-Crentsil K, Brown T, Song S. Effects of aluminates on the formation of geopolymers. *Mater Sci Eng B* 2005;117(2):163–8.
- [26] Cheng TW, Chiu JP. Fire resistant geopolymer produced by granulated blast furnace slag. *Miner Eng* 2003;16(3):205–10.
- [27] Duxson P, Mallicoat SW, Lukey GC, Kriven WM, Van Deventer JSJ. The effect of alkali and Si/Al ratio on the development of mechanical properties of metakaolin-based geopolymers. *Colloid Surf A* 2007;292(1):8–20.
- [28] Stevenson M, Sagoe-Crentsil K. Relationship between composition, structure and strength of inorganic polymers: Part 1 – metakaolin-derived inorganic polymers. *J Mater Sci* 2005;40(16):2023–36.
- [29] Havlica J, Brandstetr J, Odler I. Possibilities of utilizing solid pressured fluized bed coal combustion (PSBC) for the production of blended cement. *Cem Concr Res* 1998;28(2):299–307.